



Water vapor absorption spectroscopy and validation tests of databases in the far-infrared (50–720 cm⁻¹). Part 2: H₂¹⁷O and HD¹⁷O

E.V. Karlovets ^{a,b}, S.N. Mikhailenko ^c, A.O. Koroleva ^{a,d}, A. Campargue ^{a,*}

^a University Grenoble Alpes, CNRS, LIPhy, 38000 Grenoble, France

^b Tomsk State University, Department of Optics and Spectroscopy, 36, Lenin Avenue, 634050, Tomsk, Russia

^c V.E. Zuev Institute of Atmospheric Optics, SB, Russian Academy of Science, 1. Academician Zuev square, 634055 Tomsk, Russia

^d A.V. Gaponov-Grekhov Institute of Applied Physics of the Russian Academy of Sciences, 46 Ulyanov Str., 603950, Nizhny Novgorod, Russia

ARTICLE INFO

Keywords:

Water vapor
Far infrared
Rotational spectrum
Isotopologues

ABSTRACT

The present work is the second part of our systematic study of the absorption spectrum of the water vapor isotopologues by high resolution ($\approx 0.001 \text{ cm}^{-1}$) Fourier transform spectroscopy in the far infrared (50–721 cm⁻¹). The room temperature spectra were recorded at the AILES beam line of the SOLEIL synchrotron with an absorption pathlength of 151.75 m. Here, we consider three spectra of a water vapor sample highly enriched in ¹⁷O. Line parameters retrieved from the three spectra were combined in a global list of 4432 water lines (assigned to 4651 transitions). The spectral calibration based on a statistical matching with about 370 accurate reference line positions of H₂¹⁶O allows for line center determinations with an accuracy of $5 \times 10^{-5} \text{ cm}^{-1}$ for well isolated lines of intermediate intensity. Six water isotopologues (H₂¹⁸O, H₂¹⁶O, H₂¹⁷O, HD¹⁸O, HD¹⁶O, and HD¹⁷O) were found to contribute to the spectrum. 460 and 99 of the measured H₂¹⁷O and HD¹⁷O transitions are newly observed by absorption spectroscopy. 69 H₂¹⁷O and 20 HD¹⁷O energy values of the ground (000) and first excited (010) states are newly determined.

The present set of measured H₂¹⁷O line positions is combined with 24 literature sources to provide a list of 821 empirical energies for the first five vibrational states – (000), (010), (020), (100), and (001) – using the RITZ principle. A set of 332 rotational energies of the (000) and (010) states of HD¹⁷O is determined by merging the 465 HD¹⁷O transitions measured in the present study to eight literature sources.

1. Introduction

The aim of the present work is to improve our knowledge of the absorption spectrum of the ¹⁷O isotopologues of water vapor in the far-infrared (FIR), between 50 and 720 cm⁻¹. The considered FIR region corresponding to the rotational band of H₂O is of major importance for the Earth's radiation budget. For instance, the Far-infrared-Outgoing-Radiation Understanding and Monitoring (FORUM) mission of European Space Agency is dedicated to the “observational gap across the far-infrared (from 100 to 667 cm⁻¹), never before sounded in its entirety from space” (<https://www.forum-ee9.eu/>). The water vapor absorption being very strong in this region (line intensities up to $3 \times 10^{-18} \text{ cm/molecule}$), water absorption lines are ubiquitous and systematically “interfering” with other absorption features used to monitor other species of interest. Consequently, a prerequisite for remote sensing in the FIR is an accurate characterization of the water spectrum in this region,

including the relatively weak lines located between the strong H₂¹⁶O lines, in microwindows which may be used for monitoring atmospheric trace species. These weak lines include those of the water minor isotopologues (which are by themselves important atmospheric tracers).

Experimentally, broad-band absorption spectroscopy in the FIR region is not an easy task due to the lack of tunable sources in the region. Due to its unique properties (in particular its brightness), the synchrotron source is preferable to the traditional globar sources for Fourier transform spectroscopy (FTS) (see for instance Fig. 1 of Ref. [1]). In the fall of 2021, a one-week measurement campaign dedicated to the high resolution spectroscopy of various water isotopologues (natural, ¹⁷O and D enriched) was performed at the AILES beam line of the SOLEIL synchrotron near Paris (<https://www.synchrotron-soleil.fr/en>). This campaign followed measurements campaigns dedicated to the water vapor absorption continuum (self- and foreign-continua [1–4]) where it appeared that the sensitivity of the SOLEIL spectra recorded with a 151 m pathlength allows a gain by more than three

* Corresponding author.

E-mail address: alain.campargue@univ-grenoble-alpes.fr (A. Campargue).

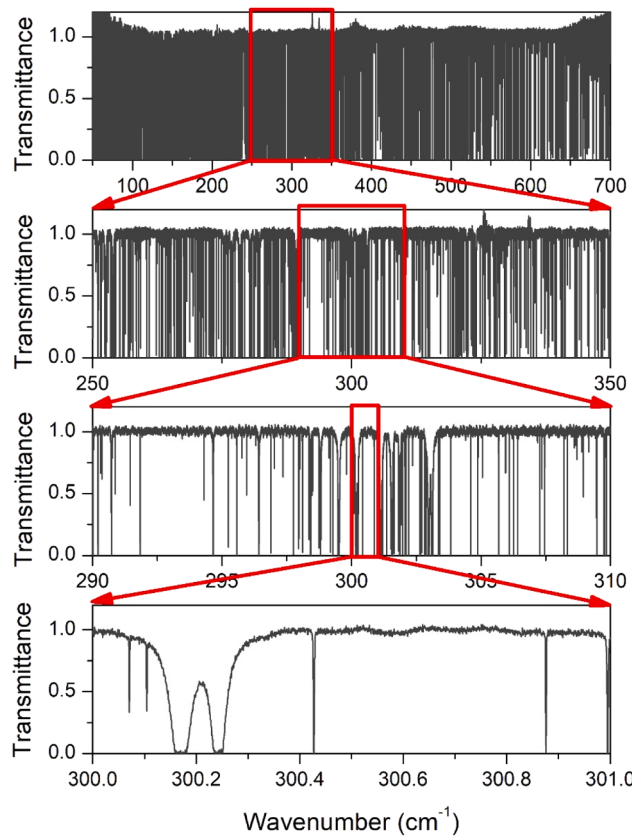


Fig. 1. Successive zooms of the FTS spectrum #7 of water vapor enriched in ^{17}O recorded at SOLEIL synchrotron at room temperature ($P \approx 0.29$ mbar) between 50 and 700 cm^{-1} .

orders of magnitude compared to previous literature studies of the main isotopologue [5]. During the 2021 measurement campaign, a total of 21 spectra were recorded at different pressures for five isotopic compositions: natural, ^{17}O enriched, D_2O , $\text{H}_2\text{O:D}_2\text{O}$ mixture, and a mixture of the ^{17}O enriched sample with D_2O . The analysis of the five spectra of the natural isotopic sample was reported in Ref. [6]. The present contribution is dedicated to the analysis of three spectra of the ^{17}O enriched sample recorded at pressures of about 29 μbar , 0.29 mbar and 3.8 mbar. (Note that the analysis of the high resolution SOLEIL spectrum of ^{18}O enriched water vapor was reported in 2020 [5] as a ‘‘side-product’’ of the SOLEIL spectra recorded for the retrieval of the H_2^{18}O self-continuum [2].)

The rest of the paper is organized as follows. In Section 2, we recall the experimental details including the spectra acquisition, line list retrieval and spectra calibration. The spectroscopic analysis is presented in Section 3 which includes an overview of the transitions contributing to the spectra together with a line position comparison with literature. In particular, we will consider (i) the HITRAN2020 spectroscopic database [7], (ii) the W2020 line lists of H_2^{16}O , H_2^{18}O and H_2^{17}O with line positions computed from empirically determined energy levels [8]. Our recommended set of H_2^{17}O energy levels up to the first triad – (000), (010), (020), (100), and (001) – is given in Section 4. New energy sets of the (000) and (010) states of HD^{17}O are also reported in this section and compared to previous studies.

2. Experiment

2.1. Spectra acquisition

The FTS spectra were acquired in September 2021 on the AILES beam line of SOLEIL synchrotron facility operated in the 500 mA multibunch mode. A Bruker 125 interferometer with a 6 μm mylar-

composite beam splitter and a 4 K cooled Si bolometer detector were used for the recordings. The absorption cell is a multipass cell in White-type configuration. The total absorption path length, L , was set to 151.75 ± 1.5 m corresponding to 60 passes between mirrors separated by 2.52 m and about 0.5 m of space between the 50 μm thick polypropylene films windows. Three spectra were recorded for pressure values of about 29 μbar , 0.29 mbar and 3.8 mbar, measured by a capacitance gage (Pfeiffer 10 mbar full range with corresponding accuracy of 0.01 mbar). The ^{17}O water sample (from Eurisotop) has a stated chemical purity better than 99.99 %. Its isotopic composition is strongly enriched in ^{17}O and to a lesser extent in ^{18}O : the oxygen isotopic abundances are 57.9, 38.2 and 1.2 % for ^{17}O , ^{16}O and ^{18}O , respectively, according to the certificate of analysis. The water sample was frozen and liquefied several times before injection in the cell. Table 1 summarizes the experimental conditions and the sequence of the recordings.

The last spectrum was recorded at very low pressure, pumping on the cell in order to measure the strongest lines (intensities up to 10^{-18} $\text{cm}/\text{molecule}$). The two lowest pressure spectra were recorded with the maximum spectral resolution of 0.00102 cm^{-1} (defined as 0.9/MOPD where MOPD = 882 cm is the maximum optical path difference). At 3.8 mbar (spectrum #8), the pressure broadening makes unnecessary to adopt the highest resolution and a spectral resolution of 0.002 cm^{-1} was adopted. The number of co-added spectra ranges between 160 and 300 (200 spectra corresponds to about 10 h acquisition time at 0.001 cm^{-1} spectral resolution or 5 h at 0.002 cm^{-1} resolution). No apodization of the interferogram was used (boxcar option of the Bruker software). The baseline fluctuations were corrected by division by a lower resolution (0.05 cm^{-1}) spectrum acquired prior to each high resolution recording (see Table 1). The temperature of 295.5(3) K was monitored by a pair of platinum sensors mounted on the cell external surface. An overview of the spectrum recorded at 0.29 mbar is displayed on Fig. 1, which includes successive zooms. The absorption coefficient was determined as $\alpha_{\text{total}}=1/L\ln(I_0(v)/I(v))$, where $L = 151.75$ m, and $I(v)$ and $I_0(v)$ correspond to the spectrum with the cell filled with water vapor and evacuated, respectively.

The present study being mainly focused on line positions, each of the three transmittance spectra was fitted independently assuming the standard Voigt line profile as line shape (with adjusted Gaussian and Lorentzian widths) and no particular care was taken for the treatment of the apparatus function. The observed line profiles result from different contributions. At 1 mbar, the pressure broadening (about $4 \times 10^{-4} \text{ cm}^{-1}$ HWHM [7]) is equivalent to the width of the apparatus function (about $3.5 \times 10^{-4} \text{ cm}^{-1}$ HWHM) while the Doppler broadening (proportional to the transition frequency) is on the order of $1.5 \times 10^{-4} \text{ cm}^{-1}$ HWHM near 100 cm^{-1} . The line parameters retrieval was performed using a homemade multiline fitting program written in LabVIEW. Fig. 2 illustrates the line profile fitting of the three spectra in a small spectral interval near 330 cm^{-1} . Our goal being to construct a global line list from the line lists retrieved at the three available pressure values, the saturated lines (transmittance at center less than a few %) were omitted from the fit when a lower pressure spectrum was available and for each line, we selected the most suitable pressure condition of the parameter determination. The (obs. – calc.) residuals included in Fig. 2 are at the noise level [~ 1 % root mean square (RMS)]. This value corresponds to a noise equivalent absorption on the order of $7 \times 10^{-7} \text{ cm}^{-1}$ and a detectivity

Table 1

Experimental conditions of the three FTS spectra of ^{17}O enriched water under analysis. The temperature was 295.5 K.

	Recording	Pressure	Resolution, cm^{-1}	Nb of scans
#7	Baseline	Pumping on the cell	0.05	200
	Sample	≈ 0.29 mbar	0.001	300
#8	Baseline	Pumping on the cell	0.05	200
	Sample	≈ 3.8 mbar	0.002	200
#9	Baseline	Pumping on the cell	0.05	200
	Sample	≈ 29 μbar	0.001	160

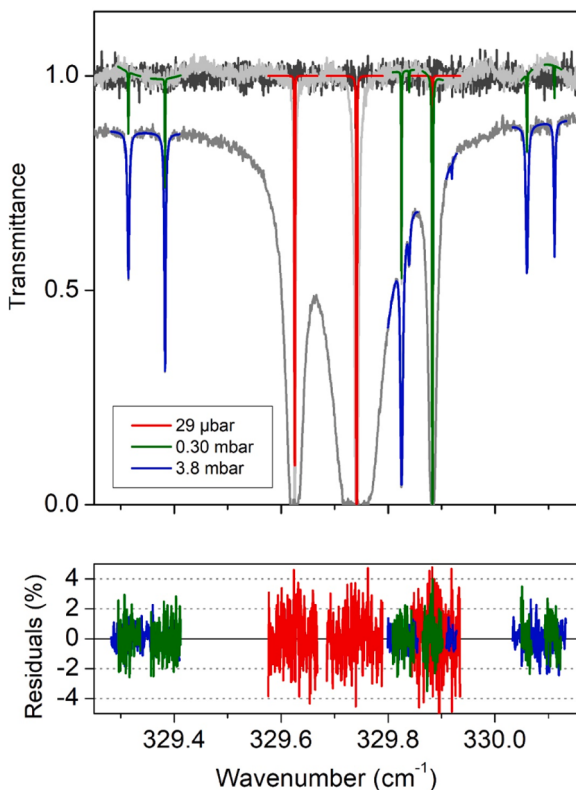


Fig. 2. Line parameter retrieval from the FTS spectra of water vapor enriched in ^{17}O near 330 cm^{-1} . The line profile fit was performed in narrow spectral intervals around the lines which are not too saturated.

Upper panel: Recorded spectra at $29\text{ }\mu\text{bar}$, 0.29 mbar and 3.8 mbar with corresponding best fit spectra (red, green and blue, respectively).

Lower panel: Corresponding $(\text{exp.} - \text{fit})$ residuals in %.

threshold of about $10^{-25}\text{ cm/molecule}$ for the line intensities measured in the 3.8 mbar spectrum.

We provide as a supplementary material the global line list of water lines obtained by combining the three individual lists. After removal of a few impurity lines (see details below), the composite list includes a total of about 4400 water lines. For each line, the spectrum used for the line parameter retrieval is indicated by the corresponding tag (#7–9). The spectra at $29\text{ }\mu\text{bar}$ (#9), 0.29 mbar (#7) and 3.8 mbar (#8) were used for 1355, 2065 and 1012 lines, respectively. The corresponding lines are plotted with different colors on the line list overview displayed in Fig. 3.

Several comments deserve to be given regarding line intensities. The isotopic composition of water vapor is not identical in the three analyzed spectra and differs significantly from the stated isotopic composition of the used ^{17}O enriched water sample. From intensity comparison to HITRAN intensity values, it appears that the H_2^{17}O relative abundance (about 34 %) is nearly twice smaller than its stated value of 57.9 % while the H_2^{18}O abundance (about 23 %) is much larger than its stated value of 1.2 %. This situation is due to the fact that the same absorption cell was previously used for spectra recordings with nearly pure H_2^{18}O [2,5]. Due to exchanges between H_2^{18}O molecules adsorbed in the walls of the cell and water molecules in the gas phase, H_2^{17}O and H_2^{18}O abundances tend to equilibrate which leads to the observed isotopic compositions (which depends on the spectrum considered). In order to provide consistent line intensities in our global line list, the H_2^{16}O , H_2^{17}O and H_2^{18}O relative abundances were determined for the three analyzed spectra and used to scale all intensity values to the following isotopic abundances (in %): 42.987 (H_2^{16}O), 33.989 (H_2^{17}O), 22.993 (H_2^{18}O), 0.013 (HD^{16}O), 0.011 (HD^{17}O) and 0.007 (HD^{18}O). Note that these values correspond to a relative natural abundance of deuterium ($\text{HD}^X\text{O}/\text{H}_2^X\text{O}$ abundance ratio of about 3×10^{-4}). The HITRAN line list

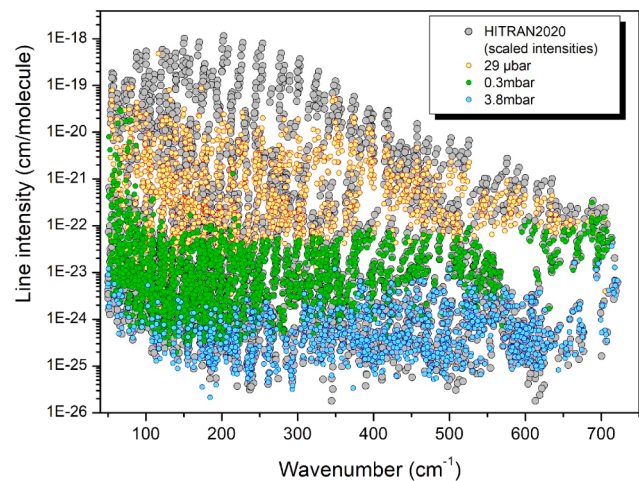


Fig. 3. Overview of the line lists retrieved from the three analyzed spectra of water vapor enriched in ^{17}O between 40 and 720 cm^{-1} . The global experimental line list was obtained by combining the lists at $29\text{ }\mu\text{bar}$, 0.29 mbar and 3.8 mbar (yellow, green and cyan circles, respectively). Note that line intensities are strongly underestimated for the low pressure spectra. Gray circles correspond to the HITRAN list with line intensities scaled according to the isotopic abundance of the sample (Table 1).

with intensity scaled according to the above isotopic composition is displayed in Fig. 3. The intensity comparison with our experimental values indicates that for the strongest lines (retrieved from the lowest pressure spectrum at $29\text{ }\mu\text{bar}$), our measured intensities are strongly underestimated. This is the consequence that lines with intensities larger than $10^{-20}\text{ cm/molecule}$ are completely saturated, even at the lowest pressure conditions of the recordings. Although of limited accuracy, these lines were kept in our global line list for completeness. For non-saturated lines, we do not claim either for a high accuracy of the intensity values. Our line intensities are believed to be reasonable in the 10^{-25} – $10^{-21}\text{ cm/molecule}$ range but several factors limit their accuracy to about 5–10 % in the best cases: small number of points describing the line profile, uncertainty on the isotopic composition and impact of the apparatus function which was roughly taken into account in the line parameter retrieval. The fit uncertainty on the line intensity included in the global line list corresponds to the value provided by the line profile fitting program and is only indicative. Our intensity accuracy is insufficient for validation tests of the calculated intensities provided by variational calculations. In the following we will thus focus on line positions (and energy levels).

2.2. Frequency calibration

The above combination of the three line lists into a single global list assumes that there is no significant variation of the frequency axis during the recordings. This assumption was validated in Ref. [6] on the basis of the spectra of natural water recorded during the same measurement campaigns as the presently analyzed spectra. The absolute frequency calibration of our global list was performed considering the lines of the spectra at $29\text{ }\mu\text{bar}$ and 0.29 mbar for which the self-pressure shift of the line positions is negligible (According to Refs. [9–15], the amplitude of the self-pressure shifts of rotational lines is less than $0.05\text{ cm}^{-1}/\text{atm}$ which leads to a maximum position shift of $1.5\times 10^{-5}\text{ cm}^{-1}$ at 0.29 mbar). We used as reference line positions the wavenumber of 223 transitions reported in Ref. [16] with an accuracy better than $1\times 10^{-6}\text{ cm}^{-1}$. The differences between the experimental line centers and the reference values were fitted as a linear function. The obtained empirical correction of the frequencies is $+7.79\times 10^{-5}$ – $-6.95\times 10^{-7}\sigma$ where σ is the measured wavenumber. A root mean square deviation of $2.5\times 10^{-5}\text{ cm}^{-1}$ was obtained for the linear fit, thus much larger than the accuracy

of the position of the reference lines. This value gives an estimate on our best accuracy on the reported line positions. In the global line list provided as Supplementary Material, the fit error on the line position determination is included. For a significant fraction of the lines, the fit uncertainty (thus excluding the frequency calibration error) was found smaller than $2.5 \times 10^{-5} \text{ cm}^{-1}$ and is thus believed to underestimate the real uncertainty on the line position. For all these lines, we replaced the fit uncertainty by a value of 3×10^{-5} , 5×10^{-5} and $1.5 \times 10^{-4} \text{ cm}^{-1}$ for the line positions retrieved from the spectra at 29 μbar , 0.29 mbar and 3.8 mbar, respectively. Note that the position uncertainty of the weakest, highly blended lines or saturated lines can reach a value of $5 \times 10^{-4} \text{ cm}^{-1}$ in the worst cases.

As concerns line intensities, as mentioned above, the fit uncertainty included in the global line list is only indicative.

3. Analysis and comparison with literature

3.1. General considerations

The HITRAN2020 rovibrational assignments of practically all observed water transitions have been validated and transferred to our list. The HITRAN rovibrational assignment of 187 high J transitions in the pure and (010)–(010) rotational bands of H_2^{17}O (from Lodi and Tennyson [17]) and 23 transitions of the same bands of H_2^{18}O (from Bubukina et al. [18]) is incomplete in the HITRAN list [4,7]. The complete assignment is provided in our list. Due to the fact that assignments of Partridge and Schwenke [19] coincide with those of the W2020 line list [8] for the main isotopologue H_2^{16}O , the missing assignments of H_2^{18}O and H_2^{17}O have been completed according those from Ref. [19].

Overall the global list includes 4935 absorption features. Among them, 430 lines are due to the impurities: 5 lines of hydrogen fluoride (HF), 109 lines of ammonia ($^{14}\text{NH}_3$ and $^{15}\text{NH}_3$) and 313 lines of the v_2 band of different isotopologues of carbon dioxide ($^{12}\text{C}^{16}\text{O}_2$, $^{13}\text{C}^{16}\text{O}_2$, $^{12}\text{C}^{17}\text{O}_2$, $^{12}\text{C}^{18}\text{O}_2$, $^{16}\text{O}^{12}\text{C}^{17}\text{O}$, $^{16}\text{O}^{13}\text{C}^{17}\text{O}$, $^{16}\text{O}^{12}\text{C}^{18}\text{O}$, $^{17}\text{O}^{12}\text{C}^{18}\text{O}$) above 640 cm^{-1} . The impurity abundances are the largest at a pressure of 0.29 mbar (#7) and estimated as 1 ppm for HF, 2 ppm for NH_3 and 140 ppm for CO_2 . More than 4600 lines are water lines assigned to the H_2^{16}O ,

HD^{16}O , H_2^{17}O , HD^{17}O , H_2^{18}O , and HD^{18}O isotopologues. Three weak lines (line intensity less than $10^{-25} \text{ cm}/\text{molecule}$) are left unassigned. More than 70 weak and overlapped lines (mostly of H_2^{16}O and H_2^{18}O) were excluded from the final list because their line parameters were better determined from the spectra of natural water and water enriched in ^{18}O analyzed in Refs. [5,6], respectively. So, the final list contains 4432 water lines assigned to 4651 transitions of the six above-listed isotopologues. The general statistics of the assigned transitions as well as the estimated abundances of the different isotopologues are given in Table 2. The maximum value of the J rotational quantum number is 21 or 22 for the non-deuterated species and 17 or 18 for the deuterated species. For comparison, absorption studies (at room temperature) prior to our analysis of SOLEIL spectra provided observations in our region up to $J_{\max} = 17$, 17 and 16 for H_2^{16}O , H_2^{18}O , and H_2^{17}O , respectively and $J_{\max} = 17$, 13 and 11 for HD^{16}O , HD^{18}O , and HD^{17}O , respectively.

We present in Table 3 a comparison to previous literature studies of the number of observations of water transitions for the different isotopologues. Prior to our studies based on SOLEIL spectra [5,6], 632 transitions of H_2^{16}O were measured by absorption between 50 and 722 cm^{-1} (see review of the previous studies in Refs. [5,6]). A total of 693 additional transitions were reported in Refs. [5,6], including 137 transitions which were not reported in previous absorption and emission investigations. In the present work based on a ^{17}O enriched sample, we observe six H_2^{16}O transitions for the first time by absorption (all of them were previously reported in emission by Coheur et al. [20] and Yu et al. [21]). Let us recall that as a general rule, line positions derived by absorption have a better accuracy than when derived from emission spectra.

As concerns H_2^{18}O , the literature review indicates that 380 and 148 transitions were determined in the 50–722 cm^{-1} region by absorption and emission, respectively (see review of previous studies in Ref. [5]). Later, 1257 transitions were obtained from the SOLEIL spectra [5,6,22], 797 being new compared to previous studies. In this investigation, we observe 53 new H_2^{18}O transitions compared to previous absorption studies. This increased the total number of distinct observed transitions to 1378.

The H_2^{17}O isotopologue is the species for which the largest amount

Table 2
Statistics of assigned water transitions.

Molecule	Natural abundance (%)	Sample abundance (%)	NT ^a	J_{\max}	$K_a \max$	Range cm^{-1}	$S_{VR \min} \text{ b}$ $\text{cm}/\text{molecule}$
H_2^{16}O	99.7317	42.987	1130	22	13	51.434 – 721.423	3.8×10^{-26}
H_2^{18}O	0.199983	22.993	1066	21	13	51.218 – 719.380	6.3×10^{-26}
H_2^{17}O	0.0371884	33.989	1150	21	14	50.535 – 717.483	4.5×10^{-26}
HD^{16}O	0.0310693	0.013	449	18	10	50.276 – 528.100	5.2×10^{-26}
HD^{18}O	6.23003×10^{-5}	0.007	391	17	10	50.032 – 475.493	5.2×10^{-26}
HD^{17}O	1.15853×10^{-5}	0.011	465	18	11	50.133 – 554.165	5.5×10^{-26}
Total			4651	22	14	50.032 – 721.423	3.8×10^{-26}

Notes.

^a Number of assigned transitions.

^b Intensity value of the weakest line.

Table 3
Statistical comparison of the number of assigned water transitions between 50 and 722 cm^{-1} .

Molecule	Prior literature ^a		Refs. [5,6]	This work		
	Absorption	Emission + absorption		Total	New in absorption	New
H_2^{16}O	632	3745	693	1130	6	0
H_2^{18}O	380	528	1168	1066	53	43
H_2^{17}O	373	373	679	1150	460	460
HD^{16}O	535	1583	688	449	1	1
HD^{18}O	207	207	1015	391	21	21
HD^{17}O	2	195	357	465	156	99
Total	2129	6631	4600	4651	697	624

Note.

^a Previous literature studies excluding those of Refs. [5,6] corresponding to the analysis of SOLEIL spectra.

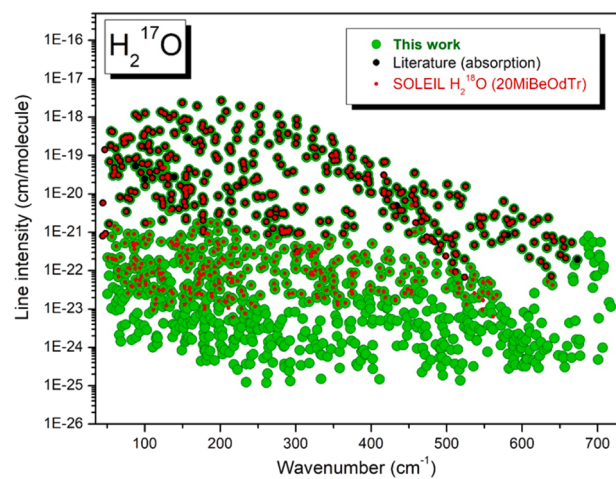


Fig. 4. Overview comparison of the H_2^{17}O line lists obtained in the present work (green circles) to previous absorption studies [23–27] (black dots) and to the line list of Ref. [5] (20MiBeOdTr) retrieved from SOLEIL spectra of ^{18}O enriched water vapor (red dots). For the sake of the comparison, the HITRAN intensity values have been adopted for all the transitions.

of new observations is provided by the present analysis. The overview comparison displayed in Fig. 4 illustrates the lowering by about two orders of magnitude of the detectivity threshold of the H_2^{17}O transitions compared to the H_2^{17}O observations in the SOLEIL spectra of ^{18}O enriched water vapor analyzed in Ref. [5]. In our region, 679 H_2^{17}O transitions were reported in Refs. [5,6] adding 320 transitions to the total set of 373 transitions reported in previous absorption studies [23–27]. In the present work, 460 additional transitions are measured increasing the total number of H_2^{17}O transitions to 1153 observations by absorption. There are no published emission data in the literature in the studied range.

For the HD^{16}O isotopologue, 688 transitions were reported in Refs. [5,6] from SOLEIL spectra adding 235 observations to the 535 absorption lines reported in the prior literature. In the present study, only the pure rotational transition $9_0\ 9 - 8_0\ 8$ at 121.9123 cm^{-1} is newly observed.

As concerns the HD^{18}O isotopologue, 895 of the 1015 transitions reported in Refs. [5,6] from SOLEIL spectra were new compared to the 207 transitions observed by Johns [28] and Yu et al. [29]. We currently observe 21 new HD^{18}O transitions which increases the total number of observed transitions to 1123 (all by absorption).

SOLEIL spectra allow for a substantial extension of the HD^{17}O dataset: 316 of the 357 HD^{17}O transitions of Refs. [5,6] were new ones compared to the prior literature (two and 193 observations by Puzzarini et al. [30] in absorption and by Mellau et al. [31] in emission, respectively). In the present work, we observe 99 additional transitions increasing the total number of HD^{17}O observations to 610.

3.2. Position comparison to the HITRAN2020 and W2020 line lists

3.2.1. H_2^{17}O

Following the approach developed by a task group (TG) of the International Union of Pure and Applied Chemistry (IUPAC-TG) [32–35], improved sets of empirical energy levels have been recently released for H_2^{16}O , H_2^{18}O and H_2^{17}O . The W2020 empirical energy levels of Ref. [8] were derived from an exhaustive collection and review (up to 2020) of measured transitions in all spectral regions. In particular, the results obtained from the analysis of the SOLEIL spectrum of highly ^{18}O enriched water vapor (Ref. [5] or 20MiBeOdTr according to the W2020 nomenclature) were taken into account for the derivation of the H_2^{17}O energy levels (in the used ^{18}O enriched sample, H_2^{17}O was enriched and has a relative abundance of nearly 1 %).

Table 4

New empirical energy levels of H_2^{17}O and HD^{17}O determined from the analysis of the absorption spectra of water vapor enriched in ^{17}O recorded between 50 and 720 cm^{-1} .

Vib	J	K_a	K_c	Energy	dE	NT
H_2^{17}O						
000	13	12	2	4065.74934	14	2
000	13	12	1	4065.74928	10	2
000	13	13	1	4325.26979	27	2
000	13	13	0	4325.26984	14	2
000	14	9	5	3671.39153	8	4
000	14	10	4	3905.64478	6	3
000	14	11	4	4152.67326	7	2
000	14	11	3	4152.67394	11	2
000	14	12	3	4409.22931	6	1
000	14	12	2	4409.22999	9	1
000	14	13	2	4672.18180	15	1
000	14	13	1	4672.18186	18	1
000	14	14	1	4938.34056	16	1
000	14	14	0	4938.34051	28	1
000	15	7	9	3614.87028	32	2
000	15	8	8	3812.85089	4	2
000	15	8	7	3813.40563	6	2
000	15	9	7	4031.08800	7	1
000	15	9	6	4031.12877	8	2
000	15	10	6	4266.42820	11	1
000	15	10	5	4266.43065	6	1
000	15	11	5	4515.28377	10	1
000	15	11	4	4515.28321	9	1
000	15	12	4	4774.36221	17	1
000	15	12	3	4774.36153	19	1
000	16	2	14	3204.14797	4	3
000	16	3	13	3430.39695	5	2
000	16	4	12	3617.76433	21	2
000	16	5	11	3753.73589	5	2
000	16	6	11	3814.35184	8	3
000	16	6	10	3864.64763	8	1
000	16	7	10	3996.57448	5	2
000	16	7	9	4007.46395	7	1
000	16	8	9	4194.54071	7	1
000	16	8	8	4195.90418	36	1
000	16	9	8	4412.75292	9	1
000	16	9	7	4412.87088	13	1
000	16	10	7	4648.89720	15	1
000	17	4	13	4010.77908	10	1
000	17	5	13	4019.54921	24	1
000	17	6	11	4286.41866	10	1
000	17	7	10	4419.78778	14	1
000	17	8	9	4601.13480	13	1
000	18	1	17	3639.32981 ^a	7	4
000	18	2	16	3931.99215	11	1
000	18	3	16	3932.02976	8	4
000	18	4	15	4193.10569	10	2
000	19	1	18	4012.25213	8	3
000	19	2	18	4012.25249	32	3
000	19	2	17	4321.64026	14	1
000	20	1	19	4402.47805	42	1
000	20	2	19	4402.47769	10	1
010	9	8	2	3737.25354	16	2
010	9	9	1	3976.58586	43	2
010	10	8	2	3982.19283	24	2
010	10	9	1	4223.11112	26	1
010	10	10	1	4476.68735	27	1
010	10	10	0	4476.68788	50	1
010	11	7	5	4025.23911 ^a	18	1
010	11	8	4	4250.49423	27	1
010	11	8	3	4250.49659	15	2
010	11	9	3	4492.89823	37	1
010	11	9	2	4492.89777	18	1
010	12	4	8	3836.90225	15	1
010	12	6	6	4114.70133	50	1
010	12	7	6	4316.06108	15	1
010	12	7	5	4316.24720	21	1
010	12	8	5	4541.89284	18	1
010	13	4	10	4065.38107	29	1
010	13	4	9	4167.24039	23	1
010	14	3	12	4175.85734	13	1

(continued on next page)

Table 4 (continued)

Vib	J	K_a	K_c	Energy	dE	NT
HD¹⁷O						
000	8	7	2	1286.95796	5	6
000	8	7	1	1286.95804	5	7
000	9	5	4	1077.48240	3	9
000	9	6	4	1237.64500	4	9
000	9	6	3	1237.64780	5	6
000	11	2	9	1137.95255	5	9
000	11	4	8	1273.25527	4	13
000	11	4	7	1282.27731	5	10
000	12	3	9	1400.64274	11	5
000	12	4	8	1476.06862	10	6
000	13	4	9	1687.62259	12	1
000	14	13	2	3956.13314	24	1
000	14	13	1	3956.13322	24	1
000	15	0	15	1623.95360	10	4
000	15	1	15	1623.95910	10	5
000	15	1	14	1807.63067	13	2
000	15	2	14	1807.86187	14	2
000	15	2	13	1963.68307	21	1
000	16	0	16	1832.90645	11	3
000	16	1	16	1832.90898	11	3

Notes: Vib $J K_a K_c$ – vibration and rotation quantum numbers; Energy – empirical term value, cm^{-1} ; dE – term value uncertainty, 10^{-5} cm^{-1} ; NT – number of transitions used for the term value determination.

^a This level is considered as a new level as its W2020 value is calculated and not empirical (see Text).

In the present work, 69 new H_2^{17}O energy levels of the ground and first excited states could be determined from the recorded spectra i.e. that they correspond to transitions tagged with “C” in the W2020 lists [8] (“C” and “M” correspond to W2020 line positions calculated by variational calculations or derived from empirically determined upper and lower energy levels using the xMARVEL procedure, respectively). The list of new energy levels is presented in Table 4. In fact, Table 4 contains term values of 71 H_2^{17}O levels. All term values are determined exclusively from rotational transitions obtained in the present study. Two of them, (000) 18₁ 17 and (010) 11₇ 5, previously reported in the W2020 energy list, have been derived from so-called “virtual transitions” (“20virt” data source in the input data set Ref. [8]), obtained from an ExoMol energy list [36]. The differences from our term values are 0.00400 and -0.06272 cm^{-1} for the (000) 18₁ 17 and (010) 11₇ 5 levels, respectively. Four observed line positions were used for the energy determination of the (000) 18₁ 17 level. The term value of the (010) 11₇ 5 level is obtained from the position of the (010) 11₇ 5 – (010) 10₆ 4 transition at 471.00805 cm^{-1} . The W2020 energies of each of the two (000) 18₁ 17 and (010) 11₇ 5 levels were determined from a single “virtual transition” (000) 18₂ 17 – (000) 18₁ 17 and (010) 11₇ 5 – (010) 11₇ 4 respectively. Thus, the W2020 energies of these levels presented are calculated and not empirical. For this reason, the corresponding values in Table 4 are given in bold italics.

We present in Fig. 5 an overview comparison of our line positions of the H_2^{17}O isotopologue to the values included in the HITRAN database, to the W2020 values and to our measured values from SOLEIL spectra of natural water (Ref. [6] or 22ToKoMiPi, not included as a W2020 source) and ¹⁸O enriched water (Ref. [5] or 20MiBeOdTr, included as a W2020 source). The empirical (M) and variational (C) W2020 line positions can be distinguished on the middle panel. The corresponding line by line position comparison is provided in the first Supplementary Material. This figure deserves several comments. Overall, the HITRAN line positions of H_2^{17}O have a poorer accuracy than the W2020 line positions in the considered spectral region. While for the H_2^{16}O and H_2^{18}O species, the W2020 line positions have been largely adopted as source for the HITRAN2020 line positions, in the case of the H_2^{17}O isotopologue, more than a half of the HITRAN values are based on empirical values determined by the IUPAC-TG [32], about fifteen years ago, and another part (781 of 1854 transitions) is based on calculated values given by Lodi and

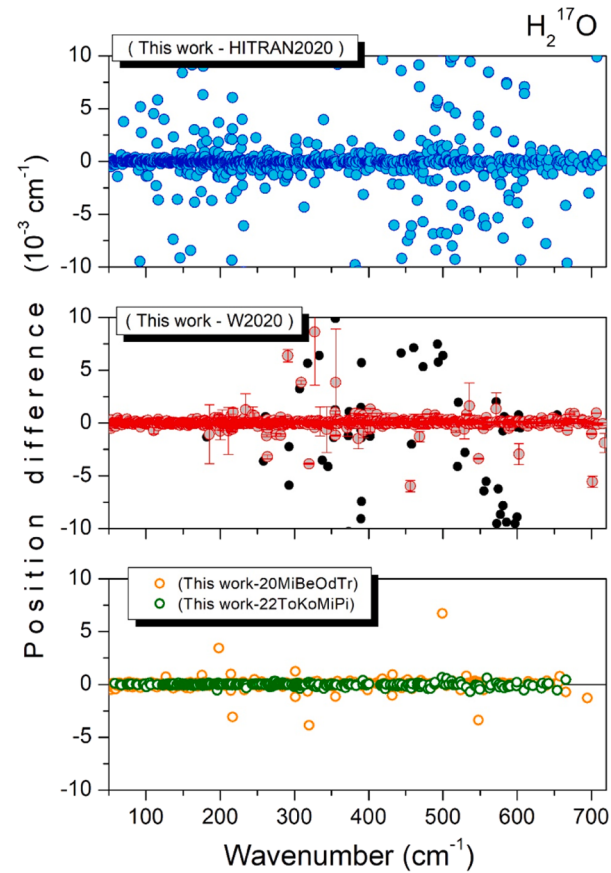


Fig. 5. Position comparison to the present measurements of the H_2^{17}O lines in the 50–720 cm^{-1} range. From top to bottom: comparison to HITRAN, W2020 (red and black dots correspond to empirical and variational levels, respectively), and our two previous analysis of SOLEIL spectra of natural water (22ToKoMiPi, Ref. [6]) (green circles) and ¹⁸O enriched water (20MiBeOdTr, Ref. [5]) (orange circles).

Tennyson [17]. Due to recent observations (in particular in 20MiBeOdTr), the W2020 set is more extensive and more accurate than the set of the IUPAC-TG [32]. In addition, part of the HITRAN line positions relies on variational energy levels (from Ref. [17]) which cannot have the experimental accuracy. Fig. 6 shows six examples for which clear deviations are observed for the HITRAN2020 line positions while W2020 positions agree with the measurements.

In order to check the consistency between our positions measurements obtained with natural, ¹⁸O enriched and ¹⁷O enriched water samples (Ref. [5], Ref. [6] and present work, respectively), on the lower panel of Fig. 5, we compare the experimental positions of these three sources. The agreement is very good: the deviations of the 20MiBeOdTr positions from the present values show a Gaussian distribution centered at $3.7 \times 10^{-5} \text{ cm}^{-1}$ with a HWHM of $6.7 \times 10^{-5} \text{ cm}^{-1}$. For 22ToKoMiPi, the corresponding values decrease to $0.9 \times 10^{-5} \text{ cm}^{-1}$ and $3.5 \times 10^{-5} \text{ cm}^{-1}$, respectively. Considering that the analyzed FIR spectra were recorded with very different isotopic samples (H_2^{17}O abundance varies from its natural value in 22ToKoMiPi, to about 1 % in 20MiBeOdTr and 47 % in the present work) and that their frequency calibration was performed independently (HITRAN reference positions in 20MiBeOdTr and 22ToKoMiPi and reference positions from Tóbiás et al. [16] in the present work), the achieved level of position agreement seems to indicate that our minimum error bars on the present position values (3×10^{-5} , 5×10^{-5} and $1.5 \times 10^{-4} \text{ cm}^{-1}$ for the spectra at 29 μbar , 0.29 mbar and 3.8 mbar) are conservative.

A small number of outliers are observed for 20MiBeOdTr. As this experimental source was part of the W2020 transitions dataset, a few

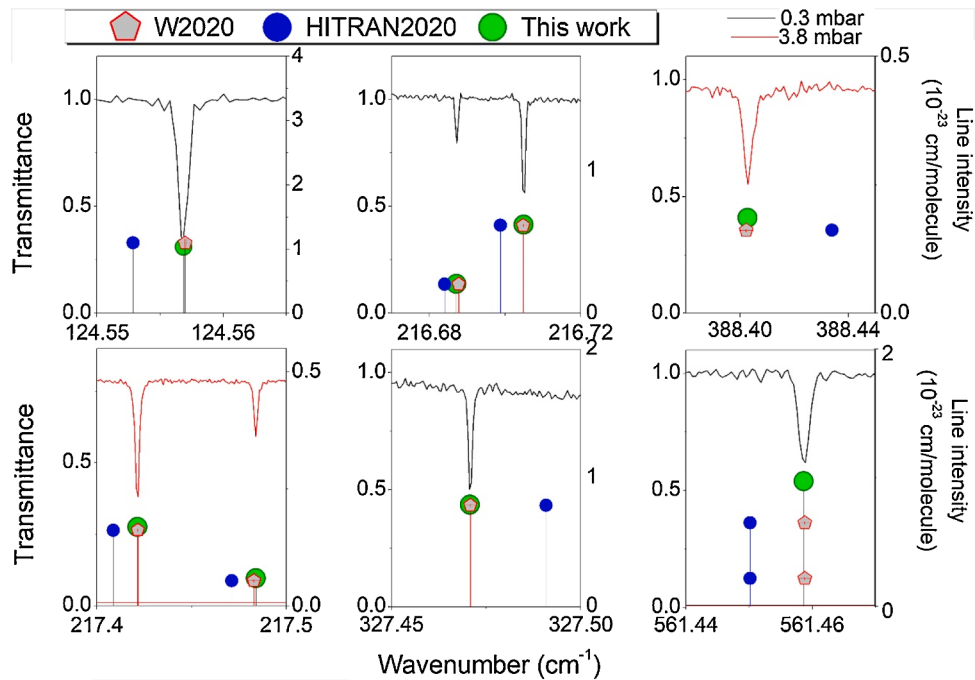


Fig. 6. Examples of inaccurate line positions in the HITRAN list.

Comparison of FTS spectra of ^{17}O enriched water vapor recorded at SOLEIL and corresponding experimental line list constructed in this work (green circles) to the W2020 and HITRAN2020 lists of H_2^{17}O (red pentagons and blue circles, respectively). All the displayed examples correspond to inaccuracies of the HITRAN2020 positions while W2020 positions agree with experiment.

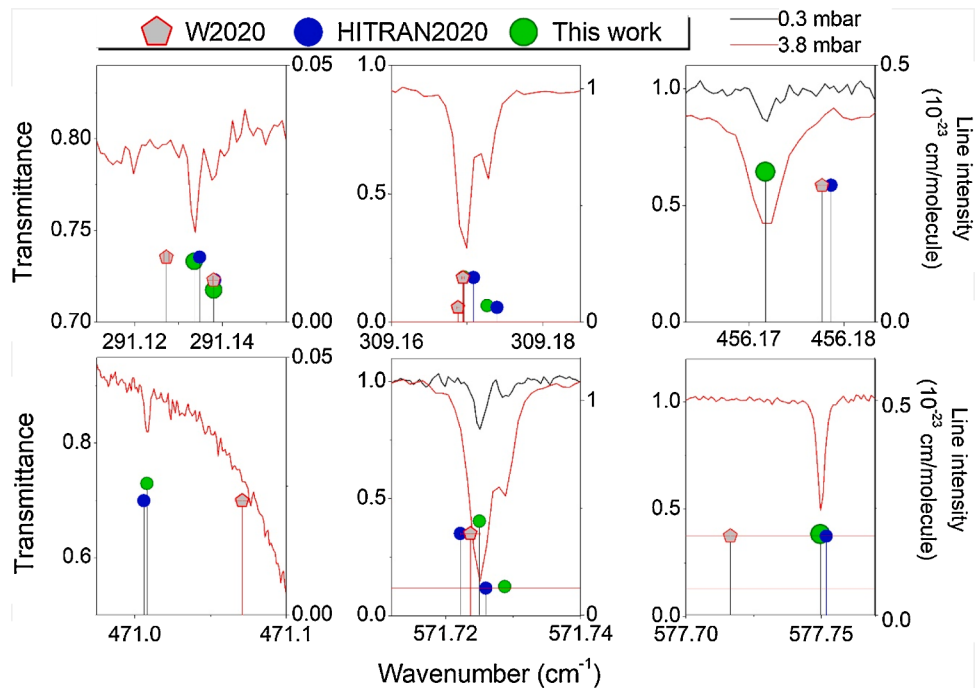


Fig. 7. Examples of inaccurate line positions in the W2020 list.

Comparison of FTS spectra of ^{17}O enriched water vapor recorded at SOLEIL and corresponding experimental line list constructed in this work (green circles) to the W2020 and HITRAN2020 lists of H_2^{17}O (red pentagons and blue circles, respectively).

W2020 inaccuracies reflect the inaccuracies in the 20MiBeOdTr dataset. However, this is not the main explanation of the large W2020 deviations which frequently exceed the W2020 claimed uncertainty. The direct comparison to the spectra presented (Fig. 7) illustrates the significance of these outliers. In some of the displayed examples, the W2020 position uncertainties (displayed on the figure) are significantly smaller than the

observed deviations. For instance, for the line displayed at $471.00805 \text{ cm}^{-1}$, the (Meas. – W2020) position difference is -0.063 cm^{-1} , 12 times larger than the claimed W2020 uncertainty ($5.1 \times 10^{-3} \text{ cm}^{-1}$ [8]). Interestingly, for two lines displayed in Fig. 7 (at 471.00805 and $577.74989 \text{ cm}^{-1}$), a much better agreement is achieved for the HITRAN position value relying on the variational values from Lodi and Tennyson

[17].

Transitions with W2020 empirical positions deviating from experiment by amount largely exceeding their W2020 uncertainties were found in our recent studies in the FIR by FTS [5,6] and in the near infrared by cavity ring-down spectroscopy (CRDS) [37–40]. These situations result from the difficulty to properly weigh the experimental line positions used to derive the W2020 energy levels. In general, extensive line lists are not provided with reliable experimental uncertainties which complicates the application of the xMARVEL procedure [8,41]. Sometimes, in particular at high energy, available high-precision data may not have a decisive influence on the determination of the corresponding W2020 energies and the resulting W2020 transition frequencies deviate from experiment.

3.2.2. HD¹⁷O

The HD¹⁷O line positions of the HITRAN2020 line list are empirical values calculated by difference of IUPAC-TG [33] empirical energy levels updated by Kyuberis et al. [42] and *ab initio* energy levels from Ref. [42]. In general, there is a good agreement between our experimental line positions and HITRAN' values. For 363 of 465 transitions the (Meas. – HITRAN2020) position differences are within 0.001 cm⁻¹. The greatest difference was found for the (000) 13₄ 9 – (000) 12₃ 10 transition, for which the *ab initio* value (345.37903 cm⁻¹, from Ref. [42]) differs from the observed value (345.49353 cm⁻¹) by -0.1145 cm⁻¹. For another ten transitions (with IUPAC-TG or variational origin) the difference exceeds 0.01 cm⁻¹.

In this investigation, we are able to observe 121 new HD¹⁷O transitions compared to our previous study [5]. For 338 transitions the (Meas. – 20MiBeOdTr) position differences do not exceed 0.00085 cm⁻¹. For the four remaining transitions, the position differences range from -0.00272 to +0.00333 cm⁻¹. The four corresponding lines in Ref. [5] are very weak and noisy lines. Two pure rotational transitions were erroneously assigned in the 20MiBeOdTr line list [5]. The line at 337.45496 cm⁻¹ was assigned to 13₅ 8 – 12₄ 9 in Ref. [5] but is not observed in the presently analyzed spectra of ¹⁷O enriched water. It is believed to be an impurity line. The real position of the 13₅ 8 – 12₄ 9 transition is 337.41736 cm⁻¹. The second one is the 13₃ 10 – 12₂ 11 transition with corrected position at 396.55543 cm⁻¹ instead of 396.56199 cm⁻¹ [5]. This last line is at the noise level in the spectrum of Ref. [5].

3.2.3. Other isotopologues

The most extensive set of absorption measurements of H₂¹⁶O transitions in the region (1310 transitions) were retrieved from the recent analysis of the natural sample, reported in Ref. [5] where a detailed comparison to the HITRAN2020 and W2020 line positions was discussed.

Here we observe a subset of 1130 H₂¹⁶O transitions (including six additional transitions not reported in Ref. [5]). For 1098 of 1130 transitions, the (Meas. – HITRAN2020) position differences are within 0.001 cm⁻¹. Only for 23 lines (30 transitions, mostly with large *J* and *K_a* values) the deviations exceed 0.001 cm⁻¹. The maximum deviations (0.00274 cm⁻¹) are observed for two pure rotational transitions: 17₂ 16 – 17₁ 17 at 309.79248 cm⁻¹ (instead of 309.78982 cm⁻¹ [7]) and 17₂ 16 – 16₁ 15 at 338.76557 cm⁻¹ (instead of 338.76283 cm⁻¹ [7]). The RMS deviation is 3.4 × 10⁻⁴ cm⁻¹ for 1128 transitions. Despite the fact that the HITRAN2020 list includes pure rotational H₂¹⁶O transitions up to *J* = 27, for an unknown reason, it does not include the 22₁ 22 – 21₀ 21 and 22₀ 22 – 21₁ 21 transitions at 407.74668 cm⁻¹ (407.74639 cm⁻¹ in Ref [6]). According to the W2020 line list [8], the intensities of these transitions are of the order of 10⁻²⁶ cm/molecule, which is significantly higher than the HITRAN intensity cutoff (1 × 10⁻³⁰ cm/molecule).

Comparison of the observed line positions with those of the W2020 line list [8] also shows very good agreement. The RMS residual of the (Meas. – W2020) position differences is 4.1 × 10⁻⁴ cm⁻¹ for 1130 H₂¹⁶O transitions. The (Meas. – W2020) position differences exceed 0.001

cm⁻¹ only for 39 transitions. The maximum deviation (0.00352 cm⁻¹) is observed for the pure rotational transition 15₁₀ 6 – 14₉ 5 at 597.88635 cm⁻¹ (instead of 597.88986 cm⁻¹ [8]). Note the (Meas. – HITRAN2020) position difference for this transition is ten times smaller (0.00029 cm⁻¹) while the W2020 source [8] is given in the HITRAN2020 database. This is one of the numerous cases where the original W2020 position value differs from HITRAN2020 value while W2020 reference is given as HITRAN source. This problem is present in all the spectral regions (see discussion in Refs. [37–40]).

The comparison of the HD¹⁶O line positions with the HITRAN2020 data gives the RMS residual of 1.7 × 10⁻⁴ cm⁻¹ for 447 transitions. All but two residuals are within 0.00072 cm⁻¹. The maximum deviations are for two pure rotational transitions: 18₀ 18 – 17₁ 17 at 234.50026 cm⁻¹ (instead of 234.49709 cm⁻¹ [7]) and 18₁ 18 – 17₀ 17 at 234.50255 cm⁻¹ (instead of 234.49912 cm⁻¹ [7]).

The (Meas. – HITRAN2020) position differences are within 0.0009 cm⁻¹ for 1042 of the 1068 measured H₂¹⁸O transitions. For 22 transitions, the deviation exceeds 0.001 cm⁻¹ with maximum deviation of 0.15 cm⁻¹ for the (010) 10₁₀ 1 – (010) 9₉ 0 transition. Most of the significant discrepancies were discussed in Ref. [5]. Firstly, the observed pure rotational transitions 21₀ 21 – 20₁ 20 and 21₁ 21 – 20₀ 20 at 388.85169 cm⁻¹ are missing in the HITRAN2020 line list. The measured positions of the 20₁ 20 – 19₀ 19 and 20₀ 20 – 19₁ 19 transitions at 371.55995 cm⁻¹ and 20₂ 19 – 19₁ 18 and 20₁ 19 – 19₂ 18 transitions at 389.44564 cm⁻¹ differ from their HITRAN (calculated) values by -0.00476, -0.00474, -0.00457, and -0.00345 cm⁻¹ respectively. Note all six above mentioned transitions are observed for the first time.

The (Meas. – W2020) position differences for 1059 H₂¹⁸O transitions are within 0.0009 cm⁻¹. Only for seven transitions these values exceed 0.001 cm⁻¹. The largest discrepancy of 0.03 cm⁻¹ is for the pure rotational transition 19₂ 17 – 18₃ 13 at 388.83421 cm⁻¹ (388.86445 cm⁻¹ in Ref. [8]). This deviation is due to an erroneous assignment of the 19₂ 17 – 19₁ 18 transition to a line at 309.00299 cm⁻¹ in Ref. [5] (used in the W2020 dataset [8]) and an incorrect value of the 19₃ 17 – 19₂ 17 “virtual transition” as 0.008388 cm⁻¹ [8]. The correct position of the 19₂ 17 – 19₁ 18 transition is 308.97269 cm⁻¹. For the 20₁ 20 – 19₀ 19, 20₀ 20 – 19₁ 19, 20₂ 19 – 19₁ 18, 20₁ 19 – 19₂ 18, and 21₁ 21 – 20₀ 20 pure rotational transitions the W2020 variational values differ by -0.00440, -0.00691, -0.00114, -0.00621, and +0.00273 cm⁻¹, respectively.

383 of the 391 measured HD¹⁸O transitions have their line positions coinciding with HITRAN values within 0.001 cm⁻¹. For eight transitions the (Meas. – HITRAN2020) position differences are between -0.00226 and 0.00373 cm⁻¹ with the biggest discrepancy for the 16₀ 16 – 15₁ 15 transition at 208.25059 cm⁻¹.

4. Energy levels

4.1. H₂¹⁷O

All but four H₂¹⁷O lines measured in the analyzed SOLEIL spectra are rotational transitions either within the ground (000) or the first excited (010) states. Consequently, we mainly focus on the determination of an improved set of empirical rotational energy values for two lowest vibrational states using both the present measurements and literature data. For this purpose, only line positions associated with the five lowest states have been taken from the literature, namely, transitions of the three rotational [(000) – (000), (010) – (010) and (020) – (020)] and five vibration-rotation (v_1 , v_2 , v_3 , $2v_2$, and $2v_2-v_2$) bands. The 1206 line positions of Refs. [5,6] and 1150 line positions of the present work of the three rotational bands were merged to more than 3600 positions of the rotational and vibration-rotation transitions of Refs. [23–27,43–57] and to about 800 unpublished line positions from FTS absorption spectra recorded by Keppler [58]. The term values and estimations of their uncertainties have been obtained using the RITZ program [59] developed by S.A. Tashkun (IAO SB RAS).

Finally, from about 6600 line positions, a total of 821 energy levels

were determined for the (000), (010), (100), (001) and (020) vibrational states. Among them, 671 and 737 are included in the IUPAC-TG [34] and W2020 [8] datasets, respectively. 296 pure rotational energies of the ground state up to $E_{\max} = 4938.34 \text{ cm}^{-1}$, $J_{\max} = 20$ and $K_a \max = 14$ and 175 rotational energies of the first excited state (010) up to $E_{\max} = 4544.66 \text{ cm}^{-1}$, $J_{\max} = 17$ and $K_a \max = 10$ were obtained. A total of 157 levels of the (000) and (010) states relies exclusively on the previous [5, 6] and present FIR spectra recorded at SOLEIL and 95 of them rely exclusively on the ^{17}O enriched spectra under analysis.

The list of energy levels and corresponding error bars are provided as a Supplementary Material including, for each level, the experimental sources used for the energy derivation. We also include in the Supplementary Material a comparison with the IUPAC-TG [34] and W2020 [8] empirical energy levels. The overview of the comparisons is presented in Fig. 8.

For 36 ground state levels, $|\delta E| = |E^{\text{TW}} - E^{\text{IUPAC-TG}}| > 0.001 \text{ cm}^{-1}$. The largest differences of the ground state energies (out of scale of the figure) are for the $13_7 6$ ($\delta E = -0.03346 \text{ cm}^{-1}$), $11_{11} 0$ ($\delta E = 0.02917 \text{ cm}^{-1}$), $11_{11} 1$ ($\delta E = 0.02893 \text{ cm}^{-1}$), $12_7 6$ ($\delta E = 0.01017 \text{ cm}^{-1}$), and $13_6 8$ ($\delta E = -0.00905 \text{ cm}^{-1}$) levels. The RMS deviation for 185 levels (excluding the five above-mentioned levels) is $9.5 \times 10^{-4} \text{ cm}^{-1}$. For 152 levels of the (010) state, the RMS is $4 \times 10^{-4} \text{ cm}^{-1}$ with a maximum discrepancy of 0.00277 cm^{-1} for the $17_0 17$ level. For comparison, the average uncertainty of our energy levels is $3.6 \times 10^{-5} \text{ cm}^{-1}$ with a standard deviation of $5.9 \times 10^{-5} \text{ cm}^{-1}$.

The comparison with the W2020 energies shows much better agreement for the ground state. The absolute deviation, $|\delta E|$, exceeds 0.001 cm^{-1} only for twelve levels with largest differences of 0.00658 and -0.00548 cm^{-1} for the $17_3 15$ and $15_6 10$ level, respectively. All other deviations are within 0.0008 cm^{-1} . The RMS deviation for 253

levels (excluding the $17_3 15$ and $15_6 10$ levels) is $5.8 \times 10^{-4} \text{ cm}^{-1}$. For the energies of the first excited state (010), the $11_7 5$ ($\delta E = -0.06272 \text{ cm}^{-1}$) and $13_3 11$ ($\delta E = 0.00638 \text{ cm}^{-1}$) levels correspond to the largest differences. In addition, $|\delta E|$ exceeds 0.001 cm^{-1} for the levels $12_3 9$ ($\delta E = -0.00288 \text{ cm}^{-1}$), $14_0 14$ ($\delta E = -0.00259 \text{ cm}^{-1}$), $15_1 15$ ($\delta E = -0.00202 \text{ cm}^{-1}$), and $10_8 3$ ($\delta E = -0.00128 \text{ cm}^{-1}$). All other deviations $|\delta E|$ are below 0.0007 cm^{-1} . The RMS deviation for 155 levels of the (010) state (excluding $11_7 5$ and $13_3 11$ levels) is $3.9 \times 10^{-4} \text{ cm}^{-1}$.

Note that for 13 levels of the ground state and 63 levels of the (010) state, the absolute value of the energy difference $|\delta E|$ is smaller for the IUPAC-TG levels [34] than for the W2020 ones [8].

Although the energy level determination of the first triad states was not the main goal of our work, the line position set used allows us to determine fifteen new (compared to Refs. [8,34]) term values of the (020), (100) and (001) states. Eight energy values of the (001) and (100) states were obtained from the line positions given by Toth [52]. Seven other term values of all three states are coming from unpublished line positions of the $2v_2$, v_1 and v_3 bands [58]. Comparison of our and W2020 energy sets shows very good agreement with $|\delta E| < 0.001 \text{ cm}^{-1}$ for 313 energies. For fourteen energies, $|\delta E|$ differences are between -0.018 and $+0.018 \text{ cm}^{-1}$ with the biggest discrepancy for the (100) $9_7 3$ and (100) $9_7 2$ energies.

Let us consider in more details, the largest $|\delta E = E^{\text{TW}} - E^{\text{W2020}}|$ deviations. Our term value $E^{\text{TW}} = 3559.53256(5) \text{ cm}^{-1}$ of the (000) $17_3 15$ level ($\delta E = 0.00658 \text{ cm}^{-1}$) was obtained from one single transition, (000) $17_3 15$ – (000) $16_2 14$ at $355.38459 \text{ cm}^{-1}$. The E^{W2020} ($17_3 15$) value of $3559.52598(55) \text{ cm}^{-1}$ was obtained from three CRDS transitions in the near infrared: $v_2 + v_3 18_5 14 - 17_3 15$ at $6187.1045 \text{ cm}^{-1}$ and $2v_2 + v_3 16_3 14 - 17_3 15$ at $6537.2080 \text{ cm}^{-1}$ [60] and $v_1 + v_3 18_3 16 - 17_3 15$ at $7470.7482 \text{ cm}^{-1}$ [61]. The first and third transitions are the only data to determine the (011) $18_5 14$ and (101) $18_3 16$ upper levels, respectively. However, to determine the (021) $16_3 14$ upper level, the $2v_2 + v_3 16_3 14 - 15_1 15$ transition at $7743.74570 \text{ cm}^{-1}$ [61] is used in addition to the second of the above mentioned transitions. The $7743.74570 \text{ cm}^{-1}$ position corresponds to a weak blended line. It seems that inaccurate position of this last line impacts the W2020 determination of both (021) $16_3 14$ and (000) $17_3 15$ levels.

The situation is similar in the next case. Our term value of the (000) $15_6 10$ level ($3435.68970(5) \text{ cm}^{-1}$) is confirmed by four consistent line positions observed in the present FIR spectra. The W2020 term value of this level ($3435.69518(56) \text{ cm}^{-1}$, $\delta E = -0.00548 \text{ cm}^{-1}$) was obtained from three CRDS transitions: $v_1 + v_2 16_7 9 - 15_6 10$ at $5843.22892 \text{ cm}^{-1}$ [62], $v_2 + v_3 16_8 9 - 15_6 10$ at $6122.5781 \text{ cm}^{-1}$ and $2v_1 14_5 9 - 15_6 10$ at $6631.6785 \text{ cm}^{-1}$ [58]. The first and second transitions are the only ones available to determine the (110) $16_7 9$ and (011) $16_8 9$ upper levels, respectively. But, for the (200) $14_5 9$ W2020 upper level, the $2v_1 14_5 9 - 14_2 12$ transition at $7521.88267 \text{ cm}^{-1}$ [61] is used in addition to the third of the above mentioned transitions. The $2v_1 14_5 9 - 14_2 12$ assignment in Ref. [61] is a second assignment (in addition to the HD ^{17}O $2v_3 12_4 8 - 11_3 9$ transition) for the line at $7521.88267 \text{ cm}^{-1}$. It seems this last line impacts the determination of the W2020 energy value of both (200) $14_5 9$ and (000) $15_6 10$ levels.

In the first excited state, the (010) $11_7 5$ level shows the largest energy difference ($E^{\text{TW}} - E^{\text{W2020}} = -0.06272 \text{ cm}^{-1}$), the W2020 value being given with a 0.005 cm^{-1} uncertainty. Our term value was obtained from the line position of the $v_2 - v_2 11_7 5 - 10_6 4$ transition $471.00805(23) \text{ cm}^{-1}$. The position of this good isolated line and consequently the energy value of the upper level are accurately determined. Note that no previous experimental data was available for this (010) $11_7 5$ level in the W2020 input file [8]. The W2020 energy value was determined from the (010) $11_7 4$ term value and the $0.005756(5000) \text{ cm}^{-1}$ position of the “quasi-transition” $v_2 - v_2 11_7 5 - 11_7 4$ transition (“20virt_S3” source) [8].

The δE difference between our and the W2020 energies of the (010) $13_3 11$ level ($3871.41252(11) \text{ cm}^{-1}$ and $3871.40614(50) \text{ cm}^{-1}$, respectively) is 0.00638 cm^{-1} . Our term value was obtained from the line position of the $v_2 - v_2 13_3 11 - 12_2 10$ transition at $291.13362(15) \text{ cm}^{-1}$. This is a weak but quite good isolated line. There is no doubt neither

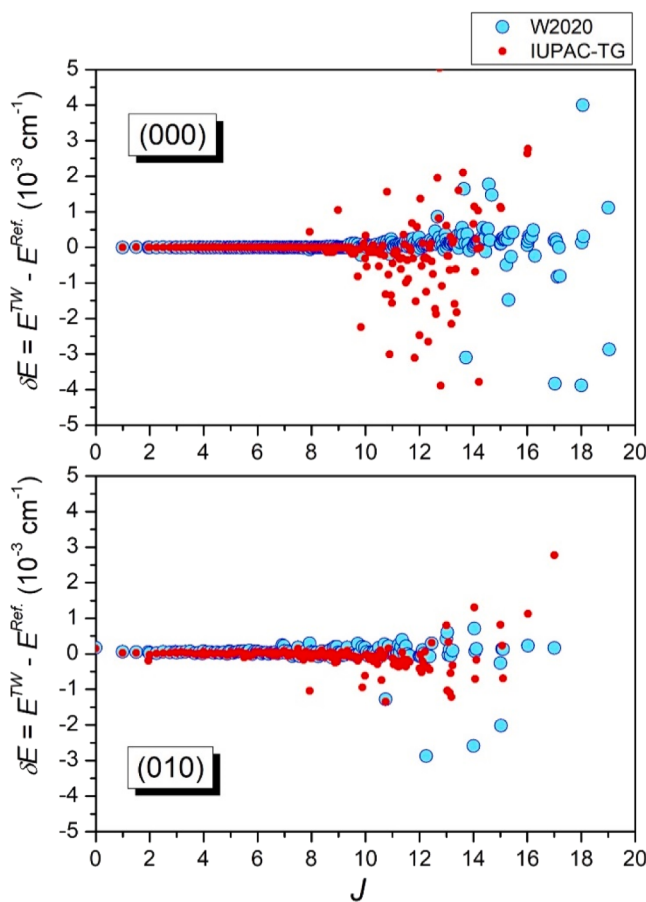


Fig. 8. Comparison of the energy levels of the ground (000) and first excited (010) vibrational states of H_2^{17}O with the IUPAC-TG and W2020 empirical values (red and blue dots, respectively).

about the position of this line nor about the energy value of the upper level. The W2020 term value was obtained from the position of the $v_2\ 13_{3\ 11} - 12_{2\ 10}$ transition at 1915.1710 cm^{-1} given by Toth [50].

4.2. HD¹⁷O

More than 2500 rotational and vibration-rotation transitions from the present study and Refs. [5,30,31,63–67] were used for the derivation of the HD¹⁷O levels in the ground and (010) vibrational states using the RITZ program [59]. In this work, we are reporting 255 pure rotation levels in the ground state up to $E_{\max} = 3770.17\text{ cm}^{-1}$, $J_{\max} = 17$ and $K_a\ \max = 13$ and 78 rotation energies of the (010) state up to $E_{\max} = 2309.26\text{ cm}^{-1}$, $J_{\max} = 11$ and $K_a\ \max = 6$. Let us recall that W2020 energy levels are not available for deuterated species. As concerns the IUPAC-TG levels of HD¹⁷O, only 86 energies of the ground ($J_{\max} = 12$) and 76 energies of the first excited ($J_{\max} = 11$) states were obtained in Ref. [33] from rotational [63,64] and v_2 [65] transitions available at that time. Later, Mellau et al. [31] (15MeMiTy) expanded the energy sets to 235 and 155 levels for the ground and first excited states, respectively. Nevertheless, some energy levels with medium and high J values and small K_a values are missing in the 15MeMiTy sets due to the weakness of the emission lines, used for the energy determination [31]. The term values of these twenty newly determined levels are included in Table 4. In addition, the precise absorption line positions obtained in the present work allow us for a general improvement of the level accuracy. The present calibration (see Section 2.2) led to a change in the energies determined from the emission line positions by values from -0.0008 cm^{-1} (for $J = 8$, $K_a = 8$) to more than 0.005 cm^{-1} (for $J = 15\text{--}17$, $K_a = 10\text{--}11$).

The complete set of the HD¹⁷O energies in the (000) and (010) states is given as a separate Supplementary Material (SP3). In addition to the term values and their uncertainties, the Supplementary Material includes comparisons to the IUPAC-TG [33] and 15MeMiTy [31] values.

5. Concluding remarks

The high brilliance and stability of the SOLEIL synchrotron radiation source combined with an absorption cell providing a 151.75-m absorption pathlength has allowed to record high quality FTS spectra of different isotopologues of water vapor in the FIR (50–720 cm^{-1}). The present study mainly devoted to the H₂¹⁷O, and HD¹⁷O isotopologues completes previous ones based on SOLEIL spectra of natural water [5] and water strongly enriched in ¹⁸O [6]. In the present work, 1150 H₂¹⁷O and 465 HD¹⁷O transitions were measured with a high position accuracy (better than $5 \times 10^{-5}\text{ cm}^{-1}$ for isolated lines of intermediate intensity) using three spectra of water vapor highly enriched in ¹⁷O (~34%) recorded at different pressures. The literature review indicates that the SOLEIL observations more than triplicate previous H₂¹⁷O observations by absorption while HD¹⁷O measurements by absorption were nearly absent (see Table 3).

The comparison to the HITRAN2020 [7] and W2020 [8] line lists of H₂¹⁷O shows a significantly better agreement for the W2020 line positions (see Fig. 6). Indeed, the W2020 empirical energy levels benefited from the extensive set of SOLEIL H₂¹⁷O line positions reported in Ref. [5] while the HITRAN line positions rely mostly on IUPAC-TG energy levels published a decade ago. We nevertheless note that a number of W2020 empirical line positions deviate from experiment by amounts exceeding their claimed uncertainties (see Fig. 7).

An important output of the present study is the derivation of 813 empirical energies for the first five vibrational states of H₂¹⁷O – (000), (010), (020), (100), and (001). The RITZ principle was applied to the present set of measured H₂¹⁷O line positions combined with 23 literature sources. The comparison to the W2020 and IUPAC-TG energy levels has been discussed with detailed considerations on a few specific levels showing the largest discrepancies. Our energy set is more complete and is believed to improve the accuracy of the W2020 dataset for the (000)

and (010) vibrational levels. For instance, the average uncertainty on our energy level values is a few 10^{-5} cm^{-1} , more than one order of magnitude smaller than the standard deviation of the $\delta E = E^{\text{TW}} - E^{\text{W2020}}$ differences.

The use of new data on rotational transitions of HD¹⁷O made it possible to newly determine the energies of 20 levels of the ground state and significantly reduce the energy uncertainties for both the ground and (010) states.

In Ref. [5], validation tests against SOLEIL spectra of natural water have illustrated the advantages of the rotation-bending Hamiltonian approach developed by Coudert et al. for the main isotopologue, H₂¹⁶O [68–70]. Overall, the predictions of this model show a nearly perfect agreement with the SOLEIL H₂¹⁶O spectra and no significant discrepancies were evidenced. Coudert et al. have recently developed a similar model for the H₂¹⁸O species and proposed a modeling of line positions and line intensities up to the first triad and $J = 20$ [22]. In the near future, based on an exhaustive literature review including the present results and some new emission data, similar theoretical approach will be applied to the H₂¹⁷O minor isotopologue.

As mentioned above, FTS spectra of water samples enriched in ¹⁷O or D (and both) were recorded during our SOLEIL measurement campaign. The analysis of the remaining spectra has been undertaken and will be reported in successive contributions. It will contribute to a better description of the water absorption spectrum in the far infrared, a spectral range of high importance for the Earth's radiation budget.

CRediT authorship contribution statement

E.V. Karlovets: Investigation. **S.N. Mikhailenko:** Investigation. **A.O. Koroleva:** Investigation. **A. Campargue:** Investigation.

Declaration of Competing Interest

The authors declare that they have no known competing financial interests or personal relationships that could have appeared to influence the work reported in this paper.

Data availability

The data are provided as Supplementary Materials

Acknowledgements

The authors are indebted to O. Pirali (ISMO) for his help during the recordings of the FIR spectra at SOLEIL synchrotron (Project No20210051). SNM activity was supported by the Ministry of Science and Higher Education of the Russian Federation (V.E. Zuev Institute of Atmospheric Optics, SB, RAS). The support of the CNRS (France) in the frame of International Research Project SAMIA is acknowledged.

Supplementary materials

Supplementary material associated with this article can be found, in the online version, at doi:10.1016/j.jqsrt.2023.108829.

References

- [1] Koroleva AO, Odintsova TA, Tretyakov MY, Pirali O, Campargue A. J Quant Spectrosc Radiat Transf 2021;261:107486. <https://doi.org/10.1016/j.jqsrt.2020.107486>.
- [2] Odintsova TA, Tretyakov MY, Zibarova AO, Pirali O, Roy P, Campargue A. Far-infrared self-continuum absorption of H₂¹⁶O and H₂¹⁸O (15–500 cm^{-1}). The foreign-continuum absorption of water vapour in the far-infrared (50–500 cm^{-1}) J Quant Spectrosc Radiat Transf 2019;227:190–200. <https://doi.org/10.1016/j.jqsrt.2019.02.012>.
- [3] Odintsova TA, Tretyakov MY, Simonova A, Ptashnik I, Pirali O, Campargue A. Measurement and temperature dependence of the water vapor self-continuum in

- the 70–700 cm⁻¹ range. *J Mol Structure* 2020;1210:128046. <https://doi.org/10.1016/j.jmolstruc.2020.128046>.
- [4] Odintsova TA, Koroleva AO, Simonova AA, Campargue A, Tretyakov MY. The atmospheric continuum in the “terahertz gap”: review of experiments at SOLEIL synchrotron and modeling. *J Mol Spectrosc* 2022;386:111603. <https://doi.org/10.1016/j.jms.2022.111603>.
- [5] Mikhailenko SN, Béguier S, Odintsova TA, Tretyakov MY, Pirali O, Campargue A. The far-infrared spectrum of ¹⁸O enriched water vapour (40–700 cm⁻¹). *J Quant Spectrosc Radiat Transf* 2020;253:107105. <https://doi.org/10.1016/j.jqsrt.2020.107105>.
- [6] Toureille M, Koroleva AO, Mikhailenko SN, Pirali O, Campargue A. Water vapor absorption spectroscopy in the far-infrared (50–720 cm⁻¹). Part 1: natural water. *J Quant Spectrosc Radiat Transf* 2022;291:108326. <https://doi.org/10.1016/j.jqsrt.2022.108326>.
- [7] Gordon IE, Rothman LS, Hargreaves RJ, Hashemi R, Karlovets EV, Skinner FM, et al. The HITRAN2020 molecular spectroscopic database. *J Quant Spectrosc Radiat Transf* 2022;277:107949. <https://doi.org/10.1016/j.jqsrt.2021.107949>.
- [8] Furtenbacher T, Tóbiás R, Tennyson J, Polyansky OL, Kyuberis AA, Ovsyannikov RI, et al. W2020: a database of validated rovibrational experimental transitions and empirical energy levels of water isotopologues. II. H₂¹⁷O and H₂¹⁸O with an update to H₂¹⁶O. *J Phys Chem Ref Data* 2020;49:043103. <https://doi.org/10.1063/5.0030680>.
- [9] Markov VN. Temperature dependence of self-induced pressure broadening and shift of the 6₄ 3–5₀ line of the water molecule. *J Mol Spectrosc* 1994;164:233–8. <https://doi.org/10.1006/jmsp.1994.1069>.
- [10] Markov VN, Krupnov AF. Measurements of the pressure shift of the 1₁ 0–1₀ water line at 556GHz produced by mixtures gases. *J Mol Spectrosc* 1995;172:211–4. <https://doi.org/10.1006/jmsp.1995.1168>.
- [11] Toth RA, Brown LR, Plymire C. Self-broadened widths and frequency shifts of water vapor lines between 590 and 2400 cm⁻¹. *J Quant Spectrosc Radiat Transf* 1998;59:529–62. <https://doi.org/10.1006/jmsp.1995.1168>.
- [12] Zou Q, Varanasi P. Laboratory measurement of the spectroscopic line parameters of water vapor in the 610–2100 and 3000–4050 cm⁻¹ regions at lower-tropospheric temperatures. *J Quant Spectrosc Radiat Transf* 2003;82:45–98. <https://doi.org/10.1006/jmsp.1995.1168>.
- [13] Podobedov VB, Plusquellec DF, Fraser GT. THz laser study of self-pressure and temperature broadening and shifts of water vapor lines for pressures up to 1.4 kPa. *J Quant Spectrosc Radiat Transf* 2004;87:377–85. <https://doi.org/10.1016/j.jqsrt.2004.03.001>.
- [14] GYU Golubiatnikov. Shifting and broadening parameters of the water vapour 183-GHz line (3₁ 3–2₂ 0) by H₂O, O₂, N₂, CO₂, H₂, He, Ne, Ar, and Kr at room temperature. *J Mol Spectrosc* 2005;230:196–8. <https://doi.org/10.1016/j.jms.2004.10.011>.
- [15] Koshelev MA, Tretyakov MY, Golubiatnikov GY, Parshin VV, Markov VN, Koval IA. Broadening and shifting of the 321-, 325- and 380-GHz lines of water vapor by pressure of atmospheric gases. *J Mol Spectrosc* 2007;241:101–8. <https://doi.org/10.1016/j.jms.2006.11.005>.
- [16] Tóbiás R, Furtenbacher T, Simkó I, Császár AG, Diouf ML, Cozijn FMJ, et al. Spectroscopic-network-assisted precision spectroscopy and its application to water. *Nat Commun* 2020;11:1708. <https://doi.org/10.1038/s41467-020-15430-6>.
- [17] Lodi L, Tennyson J. Line lists for H₂¹⁸O and H₂¹⁷O based on empirical line positions and *ab initio* intensities. *J Quant Spectrosc Radiat Transf* 2012;113:850–8. <https://doi.org/10.1016/j.jqsrt.2012.02.023>.
- [18] Zubukina II, Zobov NF, Polyansky OL, Shirin SV, Yurchenko SN. Optimized semiempirical potential energy surface for H₂¹⁶O up to 26000 cm⁻¹. *Optics and Spectroscopy* 2011;110:160–6. <https://doi.org/10.1134/S0030400X11020032>.
- [19] Partridge H, Schwenke DW. The determination of an accurate isotope dependent potential energy surface for water from extensive *ab initio* calculations and experimental data. *J Chem Phys* 1997;106:4618–39. <https://doi.org/10.1063/1.473987>.
- [20] Coheur PF, Bernath PF, Carleer M, Colin R, Polyansky OL, Zobov NF, et al. A 3000K laboratory emission spectrum of water. *J Chem Phys* 2005;122:074307. <https://doi.org/10.1063/1.1847571>.
- [21] Yu S, Pearson JC, Drouin BJ, Martin-Drumel MA, Pirali O, Vervloet M, et al. Measurement and analysis of new terahertz and far-infrared spectra of high temperature water. *J Mol Spectrosc* 2012;279:16–25. <https://doi.org/10.1016/j.jms.2012.07.011>.
- [22] Couder LH, Mikhailenko S, Campargue A, Mellau GCH. Line position and line intensity modelings of H₂¹⁸O up to the first triad and *J*=20. *J Phys Chem Ref Data* 2023;52:023105. <https://doi.org/10.1063/5.0152187>.
- [23] Winther F. The rotational spectrum of water between 650 and 50 cm⁻¹ H₂¹⁸O and H₂¹⁷O in natural abundance. *J Mol Spectrosc* 1977;65:405–19. [https://doi.org/10.1016/0022-2852\(77\)90280-6](https://doi.org/10.1016/0022-2852(77)90280-6).
- [24] Kauppinen J, Kärkkäinen T, Kyrö E. High-resolution spectrum of water vapor between 30 and 720 cm⁻¹. *J Mol Spectrosc* 1978;71:15–45. [https://doi.org/10.1016/0022-2852\(78\)90073-5](https://doi.org/10.1016/0022-2852(78)90073-5).
- [25] Kauppinen J, Kyrö E. High resolution (010) – (010) spectrum of water vapor enriched by H₂¹⁷O and H₂¹⁸O. *J Mol Spectrosc* 1980;84:405–23. [https://doi.org/10.1016/0022-2852\(80\)90032-6](https://doi.org/10.1016/0022-2852(80)90032-6).
- [26] Toth RA. Water vapor measurements between 590 and 2582 cm⁻¹: line positions and strengths. *J Mol Spectrosc* 1998;190:379–96. <https://doi.org/10.1006/jmsp.1998.7611>.
- [27] Matsushima F, Nagase H, Nakachi T, Odashima H, Takagi K. Frequency measurement of pure rotational transitions of H₂¹⁷O and H₂¹⁸O from 0.5 to 5 THz. *J Mol Spectrosc* 1999;193:217–23. <https://doi.org/10.1006/jmsp.1998.7736>.
- [28] Johns JWC. High-resolution far-infrared (20–350 cm⁻¹) spectra of several species of H₂O. *J Opt Soc Am B* 1985;2:1340–54. <https://doi.org/10.1364/JOSAB.2.0001340>.
- [29] Yu S, Pearson JC, Drouin BJ, Miller CE, Kobayashi K, Matsushima F. Terahertz spectroscopy of ground state HD¹⁸O. *J Mol Spectrosc* 2016;328:27–31. <https://doi.org/10.1016/j.jms.2016.07.005>.
- [30] Puzzarini C, Cazzoli G, Gauss J. The rotational spectra of HD¹⁷O and D₂¹⁷O: experiment and quantum-chemical calculations. *J Chem Phys* 2012;137:154311. <https://doi.org/10.1063/1.4758316>.
- [31] Mellau GCH, Mikhailenko SN, Tyuterev VLG. Hot water emission spectra: rotational energy levels of the (000) and (010) states of HD¹⁷O. *J Mol Spectrosc* 2015;308:3096–19. <https://doi.org/10.1016/j.jms.2014.12.023>.
- [32] Tennyson J, Bernath PF, Brown LR, Campargue A, Carleer MR, Császár AG, et al. IUPAC critical evaluation of the rotational-vibrational spectra of water vapor. Part I. Energy levels and transition wavenumbers for H₂¹⁷O and H₂¹⁸O. *J Quant Spectrosc Radiat Transf* 2009;110:573–96. <https://doi.org/10.1016/j.jqsrt.2009.02.014>.
- [33] Tennyson J, Bernath PF, Brown LR, Campargue A, Császár AG, Daumont L, et al. IUPAC critical evaluation of the rotational-vibrational spectra of water vapor. Part II. Energy levels and transition wavenumbers for HD¹⁶O, HD¹⁷O, and HD¹⁸O. *J Quant Spectrosc Radiat Transf* 2010;111:2160–84. <https://doi.org/10.1016/j.jqsrt.2010.06.012>.
- [34] Tennyson J, Bernath PF, Brown LR, Campargue A, Császár AG, Daumont L, et al. IUPAC critical evaluation of the rotational-vibrational spectra of water vapor. Part III. Energy levels and transition wavenumbers for H₂¹⁶O. *J Quant Spectrosc Radiat Transf* 2013;117:29–58. <https://doi.org/10.1016/j.jqsrt.2012.10.002>.
- [35] Tennyson J, Bernath PF, Brown LR, Campargue A, Császár AG, Daumont L, et al. IUPAC critical evaluation of the rotational-vibrational spectra of water vapor. Part IV. Energy levels and transition wavenumbers for D₂¹⁶O, D₂¹⁷O, and D₂¹⁸O. *J Quant Spectrosc Radiat Transf* 2014;142:93–108. <https://doi.org/10.1016/j.jqsrt.2014.03.019>.
- [36] Polyansky OL, Kyuberis AA, Lodi L, Tennyson J, Yurchenko SN, Ovsyannikov RI, Zobov NF. ExoMol molecular line lists. XIX: high-accuracy computed hot line lists for H₂¹⁸O and H₂¹⁷O. *Mon Not R Astron Soc* 2017;466:1363–71. <https://doi.org/10.1093/mnras/stw3125>.
- [37] Vasilchenko S, Mikhailenko SN, Campargue A. Water vapor absorption in the region of the oxygen A-band near 760 nm. *J Quant Spectrosc Radiat Transf* 2021;275:107847. <https://doi.org/10.1016/j.jqsrt.2021.107847>.
- [38] Campargue A, Mikhailenko SN, Kassi S, Vasilchenko S. Validation tests of the W2020 energy levels of water vapor. *J Quant Spectrosc Radiat Transf* 2021;276:107914. <https://doi.org/10.1016/j.jqsrt.2021.107914>.
- [39] Vasilchenko S, Mikhailenko SN, Campargue A. Cavity ring down spectroscopy of water vapor near 750 nm: a test of the HITRAN2020 and W2020 line lists. *Mol Phys* 2022;120:e2051762. <https://doi.org/10.1080/00268976.2022.2051762>.
- [40] Koroleva AO, Mikhailenko SN, Kassi S, Campargue A. Frequency comb-referenced cavity ring down spectroscopy of natural water between 8041 and 8633 cm⁻¹. *J Quant Spectrosc Radiat Transfer* 2023;298:108489. <https://doi.org/10.1016/j.jqsrt.2023.108489>.
- [41] Furtenbacher T, Tóbiás R, Tennyson J, Polyansky OL, Császár AG. W2020: a database of validated rovibrational experimental transitions and empirical energy levels of H₂¹⁶O. *J Phys Chem Ref Data* 2020;49:033101. <https://doi.org/10.1063/5.0008253>.
- [42] Kyuberis AA, Zobov NF, Naumenko OV, Voronin BA, Polyansky OL, Lodi L, et al. Room temperature line lists for deuterated water. *J Quant Spectrosc Radiat Transf* 2017;203:175–85. <https://doi.org/10.1016/j.jqsrt.2017.06.026>.
- [43] Steenbeckeliers G, Bellet J. Spectre micro-ondes des molécules H₂¹⁶O, H₂¹⁷O, et H₂¹⁸O. *Comp Rend Acad Sci Paris* 1971;B273:471–4.
- [44] Camy-Peyret C, Flaud JM, Guelachvili G, Amiot C. High resolution Fourier transform spectrum of water between 2930 and 4255 cm⁻¹. *Mol Phys* 1973;26:825–55. <https://doi.org/10.1080/0026897730012131>.
- [45] De Lucia FC, Helmlinger P. Microwave spectrum and ground state energy levels of H₂¹⁷O. *J Mol Spectrosc* 1975;56:138–45. [https://doi.org/10.1016/0022-2852\(75\)90210-6](https://doi.org/10.1016/0022-2852(75)90210-6).
- [46] Johns JWC, McKellar ARW. Stark spectroscopy with the CO laser: lamb dip spectra of H₂¹⁷O and H₂¹⁸O in ν_2 fundamental band. *Can J Phys* 1978;56:737–43. <https://doi.org/10.1139/p78-097>.
- [47] Partridge RH. Far-infrared absorption spectra of H₂¹⁶O, H₂¹⁷O, and H₂¹⁸O. *J Mol Spectrosc* 1981;87:429–37. [https://doi.org/10.1016/0022-2852\(81\)90414-8](https://doi.org/10.1016/0022-2852(81)90414-8).
- [48] Guelachvili G. Experimental Doppler-limited spectra of the ν_2 bands of H₂¹⁶O, H₂¹⁷O, H₂¹⁸O, and HDO by Fourier-transform spectroscopy: secondary wavenumber standards between 1066 and 2296 cm⁻¹. *J Opt Soc Am* 1983;73:137–50. <https://doi.org/10.1364/JOSA.73.000137>.
- [49] Guelachvili G, Narahari Rao K. *Handbook of infrared standards with spectral maps and transition assignments between 3 and 2600 μm*. Orlando: Academic Press; 1986. p. 851.
- [50] Toth RA. Transition frequencies and absolute strengths of H₂¹⁷O and H₂¹⁸O in the 6.2-μm region. *J Opt Soc Am B* 1992;9:462–82. <https://doi.org/10.1364/JOSAB.9.000462>.
- [51] Toth RA. 2*v*₂-*v*₂ and 2*v*₂ bands of H₂¹⁶O, H₂¹⁷O, and H₂¹⁸O: line positions and strengths. *J Opt Soc Am B* 1993;10:1526–44. <https://doi.org/10.1364/JOSAB.10.001526>.
- [52] Toth RA. The *v*₁ and *v*₃ bands of H₂¹⁷O and H₂¹⁸O: line positions and strengths. *J Mol Spectrosc* 1994;166:184–203. <https://doi.org/10.1006/jmsp.1994.1184>.
- [53] Jenouvrier A, Daumont L, Régalis-Jarlot L, Tyuterev VLG, Carleer M, Vandaele AC, et al. Fourier transform measurements of water vapor line parameters in the 4200–6600 cm⁻¹ region. *J Quant Spectrosc Radiat Transf* 2007;105:326–55. <https://doi.org/10.1016/j.jqsrt.2006.11.007>.

- [54] Puzzarini C, Cazzoli G, Harding ME, Vázquez J, Gauss J. A new experimental absolute magnetic shielding scale for oxygen based on the rotational hyperfine structure of $H_2^{17}O$. *J Chem Phys* 2009;131:234304. <https://doi.org/10.1063/1.3274062>.
- [55] Koshelev MA. Collisional broadening and shifting of the $2_1 1 - 2_0 2$ transition of $H_2^{16}O$, $H_2^{17}O$, $H_2^{18}O$ by atmosphere gases. *J Quant Spectrosc Radiat Transf* 2011;112:550–2. <https://doi.org/10.1016/j.jqsrt.2010.10.009>.
- [56] Campargue A, Mikhailenko SN, Vasilchenko S, Reynaud C, Béguier S, Čermák P, et al. The absorption spectrum of water vapor in the 2.2 μm transparency window: high sensitivity measurements and spectroscopic database. *J Quant Spectrosc Radiat Transf* 2017;189:407–16. <https://doi.org/10.1016/j.jqsrt.2016.12.016>.
- [57] Loos J, Birk M, Wagner G. Measurement of positions, intensities and self-broadening line shape parameters of H_2O lines in the spectral ranges 1850–2280 cm^{-1} and 2390–4000 cm^{-1} . *J Quant Spectrosc Radiat Transf* 2017;203:119–32. <https://doi.org/10.1016/j.jqsrt.2017.02.013>.
- [58] Keppler K. PhD Dissertation. The Ohio State University. 1995.
- [59] Mikhailenko SN, Tashkun SA, Putilova TA, Starikova EN, Daumont L, Jenouvrier A, et al. Critical evaluation of rotation-vibration transitions and an experimental dataset of energy levels of $HD^{18}O$. *J Quant Spectrosc Radiat Transf* 2009;110:597–608. <https://doi.org/10.1016/j.jqsrt.2009.01.012>.
- [60] Mikhailenko SN, Leshchishina O, Karlovets EV, Mondelain D, Kassi S, Campargue A. CRDS of ^{17}O enriched water between 5850 and 6671 cm^{-1} : more than 1000 energy levels of $H_2^{17}O$ and $HD^{17}O$ newly determined. *J Quant Spectrosc Radiat Transf* 2016;177:108–16. <https://doi.org/10.1016/j.jqsrt.2015.11.016>.
- [61] Modelain D, Mikhailenko SN, Karlovets EV, Béguier S, Kassi S, Campargue A. Comb-assisted cavity ring down spectroscopy of ^{17}O enriched water between 7443 and 7921 cm^{-1} . *J Quant Spectrosc Radiat Transf* 2017;203:206–12. <https://doi.org/10.1016/j.jqsrt.2017.03.029>.
- [62] Mikhailenko SN, Mondelain D, Karlovets EV, Kassi S, Campargue A. Cavity ring down spectroscopy of ^{17}O enriched water vapour near 1.73 μm . *J Quant Spectrosc Radiat Transf* 2019;222–223:229–35. <https://doi.org/10.1016/j.jqsrt.2018.10.027>.
- [63] Stevenson MJ, Townes CH. Quadrupole moment of O^{17} . *Phys Rev* 1957;107:635–7. <https://doi.org/10.1103/107.635>.
- [64] Steenbeckeliers G. Private communication. July 1971. (in Lovas FJ. Microwave spectral tables. II. Triatomic molecules. *J Phys Chem Ref Data* 1978;7:1445–750. <https://doi.org/10.1063/1.555588>).
- [65] Toth RA. $HD^{16}O$, $HD^{18}O$, and $HD^{17}O$ transition frequencies and strengths in the ν_2 bands. *J Mol Spectrosc* 1993;162:20–40. <https://doi.org/10.1006/jmsp.1993.1266>.
- [66] Mikhailenko SN, Naumenko OV, Nikitin AV, Vasilchenko IA, Liu AW, Song KF, et al. Absorption spectrum of deuterated water vapor enriched by ^{18}O between 6000 and 9200 cm^{-1} . *J Quant Spectrosc Radiat Transf* 2012;113:653–69. <https://doi.org/10.1016/j.jqsrt.2012.02.009>.
- [67] Liu AW, Naumenko OV, Kassi S, Campargue A. CW-cavity ring down spectroscopy of deuterated water in the 1.58 μm atmospheric transparency window. *J Quant Spectrosc Radiat Transf* 2014;138:97–106. <https://doi.org/10.1016/j.jqsrt.2014.02.002>.
- [68] Couder LH. Analysis of the rotational levels of water and determination of the potential energy function for the bending ν_2 mode. *J Mol Spectrosc* 1994;165:406–25. <https://doi.org/10.1006/jmsp.1994.1144>.
- [69] Couder LH. Analysis of the line positions and line intensities in the ν_2 band of the water molecule. *J Mol Spectrosc* 1997;181:246–73. <https://doi.org/10.1006/jmsp.1996.7171>.
- [70] Couder LH, Pirali O, Vervloet M, Lanquetin R, Camy-Peyret C. The eight first vibrational states of the water molecule: measurements and analysis. *J Mol Spectrosc* 2004;228:471–98. <https://doi.org/10.1016/j.jms.2004.04.014>.